Structure of the Rutile TiO_{2}(011) Surface in an Aqueous Environment

U. Aschauer and A. Selloni

Phys. Rev. Lett. **106**, 166102 — Published 20 April 2011

DOI: 10.1103/PhysRevLett.106.166102

The structure of the rutile TiO_2(011) surface in aqueous environment

U. Aschauer,[1] A. Selloni[1]
[1]*Department of Chemistry, Princeton University, Frick Laboratory, Princeton NJ 08544, USA*

First principles simulations are carried out to investigate the structure and stability of the rutile TiO_2(011) surface in contact with liquid water. Whereas this surface exhibits a (2×1) reconstruction in vacuo, our results show that the interaction with water leads to an inversion of the stabilities of the reconstructed and unreconstructed surfaces. This indicates that surface structures determined in vacuo or at low water coverages are not generally representative of those occurring in the aqueous environments typical of most photocatalytic applications of TiO_2.

Understanding how the surface structure of materials changes in different surrounding environments is of fundamental and practical interest. TiO_2 is widely used in photocatalysis and its surfaces play a key role in the photocatalytic properties and applications of this material [1-3]. This has lead to numerous studies of the detailed atomic scale geometries of TiO_2 surfaces in recent years [4]. These studies have revealed that, similar to most metal and semiconductor surfaces [5], TiO_2 surfaces are not simple bulk terminations, but often exhibit a reconstruction with an increased periodicity relative to that of the "ideal" bulk-terminated surface [4]. These structures, however, have generally been observed in vacuo, whereas most applications of TiO_2 involve instead an aqueous environment [1-3]. Therefore, an important question concerns the fate of the surface reconstruction in such an environment [6]. More specifically, does the surface remain the same as in vacuo? If not, how does it change? Answering these questions is essential for understanding the photoreactivity of TiO_2 surfaces and nanoparticles in aqueous solution.

In this work we address these questions for the case of rutile TiO_2(011) , the second most frequent surface in the equilibrium shape of rutile crystals [4], which has recently attracted attention because of its distinct photocatalytic activity in comparison to the widely studied rutile TiO_2(110) surface [7,8]. The bulk-terminated TiO_2(011)-(1×1) surface is shown in Fig. 1(a). We can see an undulated profile with exposed 2-fold oxygens (O_{2c}) at the apices, 5-fold Ti atoms (Ti_{5c}) at each sides, and 3-fold O (O_{3c}) at valleys. This (1×1) surface has never been observed experimentally, however. Instead, the surface is (2×1)-reconstructed in vacuo, and its structure has been recently resolved by surface X-ray diffraction (SXRD) and Scanning Tunneling Microscopy (STM) measurements in combination with Density Functional Theory (DFT) calculations [9,10]. The reconstructed surface is characterized by a corrugated profile with

alternating valleys and ridges running along the $[01\bar{1}]$ direction [see Fig. 1(b)]. There are inequivalent O_{2c} atoms on top of the ridges and forming ridge-valley bridges, and inequivalent Ti_{5c} atoms on the ridges, bonded to the ridge O_{2c} atoms, as well as at the bottom of the valleys. The computed transformation pathway from the (1×1) unreconstructed to the (2×1)-reconstructed surface is shown in Fig. 1(c) [see also the Supplementary Information]. It is a complex pathway which involves the breaking of four Ti-O bonds per (2×2) surface supercell (two on each of the ridges on the non-reconstructed surface) and an energy barrier of ~ 1.6 eV, and ultimately leads to a substantial energy gain, in agreement with the observed stability of the reconstructed surface in vacuo.

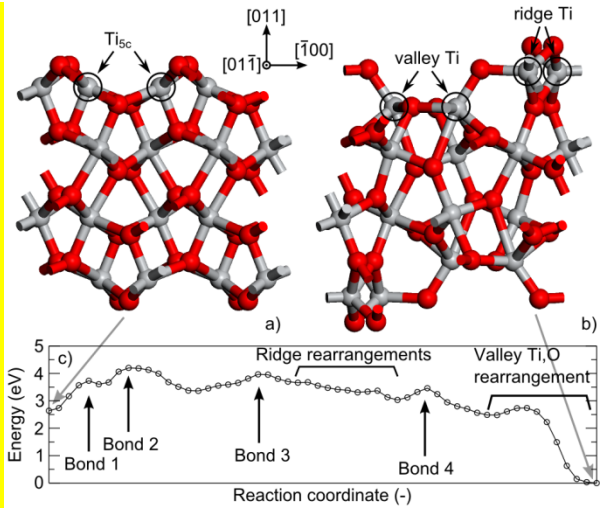

FIG. 1 Slab models of the rutile TiO_2(011) surface: (a) unreconstructed (1×1) surface; (b) (2×1)-reconstructed surface. The view is along the $[01\bar{1}]$ direction. Arrows indicate undercoordinated Ti sites. Color code: Ti = grey and O = red. (c) Potential energy profile along the (1×1) → (2×1) reconstruction pathway of a single side of the slab, as obtained by a multi-segment NEB calculation in a (2×2) surface supercell (twice the size of a (2×1) unit cell). The total energy gain in the reconstruction is ~ 2.60 eV/(2×2) cell, i.e. 1.30 eV/(2×1) cell. The arrows indicate the breaking of Ti-O bonds. Various rearrangement stages are also indicated.

The aim of this work is to theoretically determine the structure of TiO_2(011), and in particular the stability of the (2×1)-reconstructed surface, when in contact with an aqueous environment similar to that present in many real-life applications of TiO_2. Our study is based on DFT in the Generalized Gradient Approximation (GGA) of Perdew, Burke and Ernzerhof [11], and the plane wave pseudopotential scheme as implemented in the Quantum ESPRESSO package [12]. The GGA is known to be affected by the self-interaction error [13], which can be significantly reduced by applying the "+U" correction or using hybrid-functionals [14]. For the present stoichiometric surface, however, the electronic states of interest (see below) are already well localized at surface sites, so that the higher computational cost of the above methods does not seem justified. We performed total energy (static) calculations for the bulk-terminated and

reconstructed surfaces in vacuo, and first principles molecular dynamics (FPMD) [15] simulations for the same surfaces in water. We used ultrasoft [16] pseudopotentials with Ti(3s, 3p, 3d, 4s), O(2s, 2p) and H(1s) valence electrons, and expanded the wave functions in plane waves up to a kinetic energy cutoff of 35 Ry (200 Ry for the augmented density). TiO_2(011) surfaces were modeled using a repeated symmetric 4-layer (~9 Å thick) slab geometry with a 2×2 surface supercell (9.188 × 10.929 $Å^2$), corresponding to 32 TiO_2 units per simulation cell. The separation between consecutive slabs was 20 Å. Reciprocal space sampling was restricted to the Γ-point. Geometry optimizations were carried out via damped dynamics until residual forces were smaller than 0.05eV/Å. Reaction pathways in vacuo [e.g. Fig. 1(c)] were determined via climbing image Nudged Elastic Band (NEB) [17] calculations. All atoms of the slab were allowed to move/relax, and the convergence of the computed properties, e.g. adsorption energies, with respect to the slab thickness was verified.

The adsorption energies of an isolated water molecule at the exposed Ti_{5c} sites of the non-reconstructed and reconstructed TiO_2 (011) surface are reported in Table I. Water adsorption at valley sites of the reconstructed surface is about two times more favorable than on the ridge. (The valley site was not considered in a previous study of 1D water cluster formation on the reconstructed surface [18].) More intriguing is however the very large difference in adsorption energies between the non-reconstructed and the reconstructed surface. The latter is much less reactive, consistent with its lower surface energy [10], i.e. higher stability, in vacuo. Moreover, while on the non-reconstructed surface it is possible to adsorb a full monolayer of water (i.e. 1 H_2O per exposed Ti site) with an adsorption energy ΔE_{ads} = -1.04 eV per molecule (see below), on the reconstructed surface only a half-monolayer of water binds directly to surface Ti sites. The remaining water molecules adopt configurations with hydrogen bonds either with surface O atoms or with other water molecules because these interactions are stronger than the weak adsorption at ridge sites.

TABLE I. Adsorption energy, $\Delta E_{ads,}$ for a water molecule (1/8 ML coverage) at different sites on the non-reconstructed and (2×1)-reconstructed (011) rutile surface.

Non-reconstructed		**(2x1) reconstruction**	
Ti site	**ΔE_{ads} [eV]**	**Ti site**	**ΔE_{ads} [eV]**
Ti_{5c}	-1.27	Ridge	-0.21
		Valley	-0.42

We can obtain insights into the different reactivities of the non-reconstructed and (2×1)-reconstructed surfaces by considering their electronic densities of states (DOS) and partial DOS (PDOS) both in the absence ("dry" surface) and in the presence ("wet" surface) of an adsorbed water monolayer (Fig. 2). The DOS of the dry non-reconstructed surface (Fig. 2(a)) shows two small peaks just above the main edge of the valence band, which are present also after adsorption of one water monolayer at surface Ti_{5c} sites (Fig. 2(b)). These peaks, not observed on stable TiO_2

surfaces such as rutile (110) and anatase (101) [19,20], correspond to destabilized O 2p states on the ridge and valley oxygens of the surface (as determined from the layer resolved PDOS), and are likely responsible for the high reactivity of the non-reconstructed surface. On the other hand, the PDOS of adsorbed water on the reconstructed surface, Fig. 2(d), shows states at significantly higher energy relative to those on the unreconstructed surface, Fig. 2(b). This feature indicates that the electronic states of water are less stable on the reconstructed surface, consistent with the low value of the water adsorption energy on this surface.

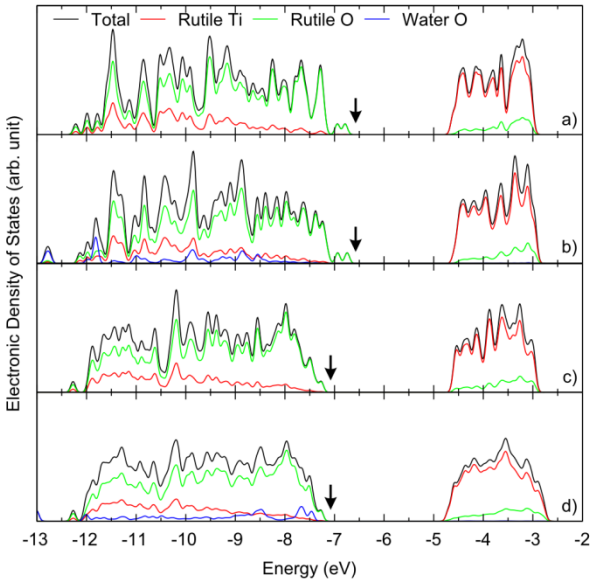

FIG. 2 Total and partial densities of states for: a) the clean non-reconstructed surface: b) the non-reconstructed surface with 8 adsorbed water molecules (one monolayer) at the Ti surface sites; c) the dry reconstructed surface, and d) the reconstructed surface with 8 adsorbed water molecules (only four of them bonded to surface Ti sites). Arrows indicate the Fermi energy. Energy scales have been aligned at the vacuum level (energy zero).

To investigate the structure of the rutile (011) in water, we carried out FPMD simulations [15] on both the unreconstructed and reconstructed TiO_2(011) slab models shown in Fig. 1. The region between consecutive slabs was filled with 64 water molecules so as to achieve a density close to that of bulk water at normal conditions. The FPMD equations of motion were integrated using a timestep of 5 a.u., a fictitious electron mass of 500 a.u., and a mass of 2 AMU for the hydrogen atoms. A Nosé-Hoover thermostat was introduced to impose a temperature of 360 K. The initial water configuration was taken from a well equilibrated FPMD simulation of bulk water at the same temperature and further equilibrated for 2 ps.

Fig. 3 shows the total potential energy evolution for the two slabs with their surrounding water environments during a run of over 20 ps after 2ps of initial equilibration. We notice a decrease of

the potential energy of the non-reconstructed surface over the first 5 ps of the run. This decrease is associated with the formation of an ordered water monolayer structure (Fig.4), implying that our initial run of 2 ps is too short for full equilibration. Despite this limitation, the probability distributions in Fig. 3 clearly shows that the total potential energy of the non-reconstructed slab with the surrounding water is on average almost 2 eV lower than the one for the reconstructed slab with water. Since the reconstructed slab was about 2.6 eV/(2×2) cell more stable in the dry state (Fig. 1c), this result is an unambiguous indication that the relative stabilities of the reconstructed and non-reconstructed surface terminations are reversed in the presence of water. A marked effect of water adsorption on the surface stability has been reported also for the Θ-alumina $(10\bar{2})$ surface [21], suggesting that water could have a similarly important role on the structure of other oxide surfaces as well.

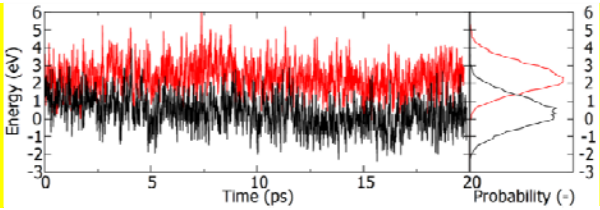

FIG. 3 Total potential energy evolution and corresponding probability distribution during 20ps FPMD simulations for the non-reconstructed (black) and reconstructed (red) slabs with their surrounding liquid water (64 molecules) environments. The results refer to a (2×2) surface supercell twice the size of a (2×1) unit cell.

To better understand the interaction of water with the bulk-terminated surface, it is useful to focus on a single adsorbed monolayer. Figure 4 shows the structure of the ordered monolayer of adsorbed water on the unreconstructed surface. In the T=0K relaxed structure (Fig. 4(a)), the water molecules are adsorbed with alternating orientations at Ti_{5c} sites (ΔE_{ads} = -1.04 eV/molecule). During the simulation, however, a constant dissociation/re-association of water molecules occurred, leading to an apparent mixed molecular/dissociated adsorption state (Fig. 4(b)). The pathway of water dissociation was investigated by a NEB calculation in which the initial and final states were the fully molecular monolayer and a monolayer with one out of 8 molecules dissociated respectively. The energy evolution and selected images along the pathway are shown in Fig. 4(d). We can see that water dissociation is accompanied by an overall small increase in energy, less than 0.1 eV [22]. Also the energy barrier for dissociation is smaller than 0.1 eV, and can thus be readily overcome at room temperature. This should favor a mixed molecular/dissociated adsorption state, slightly higher in energy but entropically preferable at finite temperature, consistent with the results of the FPMD simulations, where on average 25% of the water molecules are dissociated (Fig. 5d)).

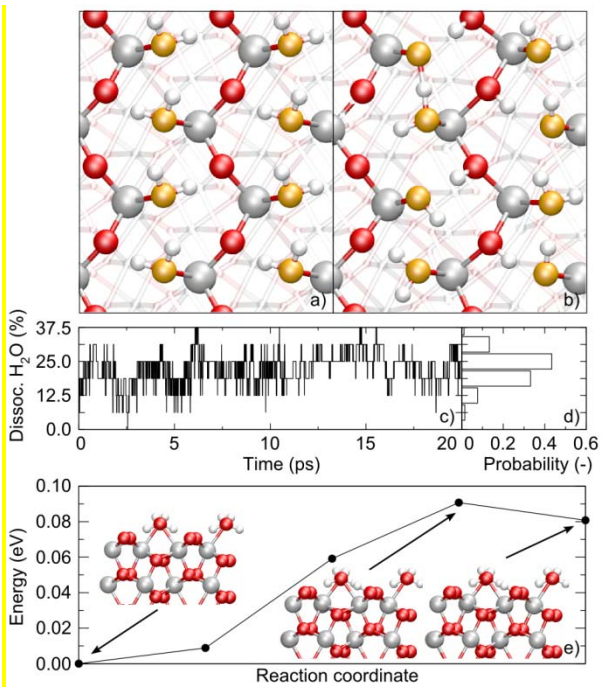

FIG. 4 a) Fully relaxed water monolayer on the non-reconstructed surface, b) typical snapshot (only first water layer shown), and c) fraction of dissociated water molecules during the 360K FPMD trajectory. Panel d) shows the energy evolution and structures during a single water dissociation NEB calculation. Color code: Ti=grey, O=red, for clarity in a) and b) water O is shown in orange and lower TiO_2 layers are shown translucent. The results refer to a (2×2) surface supercell twice the size of a (2×1) unit cell.

Turning again to Fig. 3, we can see a few very large fluctuations in the potential energy evolution of the reconstructed surface in water. We found that these fluctuations are generally associated with water dissociation events similar to the one shown in Fig. 5 (corresponding to the energy drop around 13 ps in Fig. 3). Two water molecules simultaneously bind to the same valley Ti site, one of them dissociates and the proton rapidly migrates via the Grotthuss shuttle mechanism to a ridge O site, where it forms a bridging hydroxyl group. In some cases the proton, instead of diffusing to the ridge O site, remains in solution where it forms a hydronium (H_3O^+) ion. At the same time, the OH fragment forms a tighter bond with the valley Ti atom, which then undergoes a strong outward relaxation. The simultaneous binding of two water molecules to a valley Ti site on the reconstructed surface appears to be essential for the water dissociation process. This is consistent with the fact that the energy of water dissociative adsorption is -0.29 eV for an isolated molecule, whereas, due to hydrogen bond formation, it is -0.50 eV when a second water molecule is present.

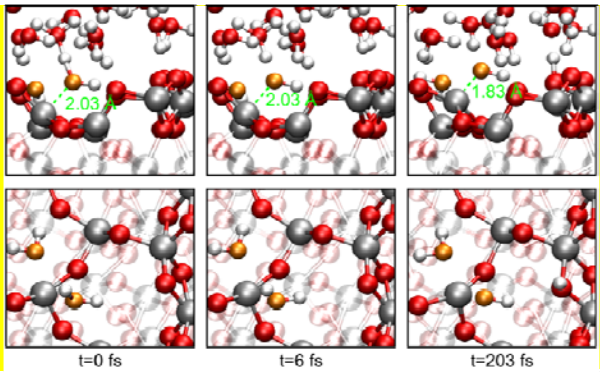

FIG. 5 Front views (top row) and top views (bottom row) of a water dissociation event at a valley Ti site with subsequent outward relaxation of the Ti atom, shortening of the Ti-OH bond and migration of the H fragment to a ridge oxygen. Water O atoms bound to the Ti site are shown in orange. For clarity subsurface layers of the slab are transparent and the water over-layer has been omitted in the top views.

In addition to the large total energy difference shown in Fig. 3, these dissociation events and the accompanying local surface restructuring indicate an instability of the reconstructed surface in presence of water. These events are rare on the timescale of our FPMD simulations (one event on the top and two events on the bottom surface of the slab in 20 ps). In order to increase their frequency and better understand their effect on the surface structure, we performed an additional simulation raising the temperature to 800K. The observed processes were essentially the same as at 300K and lead on one of the surfaces of the slab to the formation of a structure with three out of four Ti valley sites relaxed outward, which showed a remarkable resemblance to the structure of the zigzag O ridge on the non-reconstructed surface. This structure remained stable within a simulation time of 25 ps. From these observations, it seems reasonable to conclude that the rutile TiO_2(011)-(2×1) reconstructed surface can undergo a 'slow' (relative to the scale of our simulations) reverse transformation to the (1×1) bulk-terminated structure if exposed to an aqueous environment. In addition, this transformation could involve a series of dissociation/relaxation processes analogous to the one sketched in Fig. 5.

In summary, in this letter we have provided evidence that the rutile TiO_2(011) surface adopts different structures, depending on the surrounding environment. While this surface is (2×1)-reconstructed in vacuo, in the presence of bulk liquid water a bulk-like (1×1) structure is stabilized by the formation of a monolayer of tightly bound water molecules at the undercoordinated surface Ti sites. These results are not only important to improve our understanding of this particular TiO_2 surface, but more generally indicate that surface structures in vacuo and/or at low water coverage can be very different from those present in real photocatalytic applications [26]. Our study also shows that first principles simulations can contribute to bridge some of the gaps between surface science experiments and (photo)catalysis.

We thank Hongzhi Cheng for participation in the early stages of this project. This work was supported by DoE-BES, Chemical Sciences, Geosciences and Biosciences Division, Contract No. DE-FG02-05ER15702. We used resources of the National Energy Research Scientific Computing Center (DoE Contract No. DE-AC02-05CH11231), and of the center for Nanoscale Materials (DoE-BES contract No. DE-AC02-06CH11357). We also acknowledge use of the TIGRESS high performance computer center at Princeton University.

[1] A. L. Linsebigler, G. Q. Lu, and J. T. Yates, Chem. Rev. 95, 735 (1995).

[2] M. Grätzel, Nature 414, 338 (2001).

[3] A. Fujishima, X. T. Zhang, and D. A. Tryk, Surf. Sci. Rep. 63, 515 (2008).

[4] U. Diebold, Surf. Sci. Rep. 48, 53 (2003).

[5] A. Zangwill, Physics at surfaces (Cambridge University Press, Cambridge, UK, 1988).

[6] A. Selloni, Nature Materials 7, 613 (2008).

[7] J. B. Lowekamp et al., J. Phys. Chem. B 102, 7323 (1998).

[8] T. Ohno, K. Sarukawa, and M. Matsumura, New J Chem 26, 1167 (2002).

[9] X. Torrelles et al., Phys. Rev. Lett. 101 (2008).

[10] X. Q. Gong et al., Surf. Sci. 603, 138 (2009).

[11] J. P. Perdew, K. Burke, and M. Ernzerhof, Phys. Rev. Lett. 77, 3865 (1996).

[12] P. Giannozzi et al., J. Phys. Cond. Mat. 21, 395502 (2009).

[13] A. J. Cohen, P. Mori-Sanchez, and W. T. Yang, Science 321, 792 (2008).

[14] E. Finazzi et al., J Chem Phys 129, 154113 (2008).

[15] R. Car, and M. Parrinello, Phys. Rev. Lett. 55, 2471 (1985).

[16] D. Vanderbilt, Phys. Rev. B 41, 7892 (1990).

[17] G. Henkelman, B. P. Uberuaga, and H. Jónsson, Journal of Chemical Physics 113, 9901 (2000).

[18] Y. B. He et al., J. Phys. Chem. C 113, 10329 (2009).

[19] A. Tilocca, and A. Selloni, Chem. Phys. Chem. 6, 1911 (2005).

[20] U. Aschauer, J. Chen, and A. Selloni, PCCP 12, 12956 (2010).

[21] Z. Łodziana, N. Y. Topsøe, and J. K. Nørskov, Nature Materials 3, 289 (2004).

[22] Previous studies found the fully dissociated monolayer to be significantly more stable than the molecular one [23]. The PW91 functional used there, however, has been shown to yield a description of hydrogen bonding less satisfactory than the PBE functional used in this work [24,25].

[23] A. S. Barnard, P. Zapol, and L. A. Curtiss, J Chem Theory Comput 1, 107 (2005).

[24] B. Santra, A. Michaelides, and M. Scheffler, J Chem Phys 127 (2007).

[25] L. Rao et al., J Chem Theory Comput 5, 86 (2009).

[26] H. J. Freund et al., Top Catal 15, 201 (2001).